Polymicrobial Synergy Stimulates Porphyromonas Gingivalis Survival And Gingipain Expression In A Multispecies Subgingival Community

Julia R. Davies (Julia.Davies@mau.se)
Malmö University
Trupti Kad
Malmö University
Jessica Neilands
Malmö University
Bertil Kinnby
Malmö University
Zdenka Prgomet
Malmö University
Torbjörn Bengtsson
Örebro University
Hazem Khalaf
Örebro University
Gunnel Svensäter
Malmö University

Research Article

Keywords: Microbial community, Periodontitis, Dysbiosis, Virulence, Proteolytic activity

Posted Date: September 13th, 2021

DOI: https://doi.org/10.21203/rs.3.rs-842362/v1

Polymicrobial synergy stimulates *Porphyromonas gingivalis* survival and gingipain expression in a multi-species subgingival community

Julia R. Davies[1]*, Trupti Kad[1], Jessica Neilands[1], Bertil Kinnby[1], Zdenka Prgomet[1], Torbjörn Bengtsson[2], Hazem Khalaf[2] & Gunnel Svensäter[1]

[1]Section for Oral Biology and Pathology, Faculty of Odontology and Biofilms Research Center for Biointerfaces, Malmö University, Malmö S-20506, Sweden

[2]School of Medical Sciences, Örebro University, Örebro, Sweden

*Corresponding author. Telephone: +46 40 6658492, email: Julia.Davies@mau.se

Abstract

Background

Dysbiosis in subgingival microbial communities, resulting from increased inflammatory transudate from the gingival tissues, is an important factor in initiation and development of periodontitis. Dysbiotic communities are characterized by increased numbers of bacteria that exploit the serum-like transudate for nutrients, giving rise to a proteolytic community phenotype. Here we investigate the contribution of interactions between members of a sub-gingival community to survival and development of virulence in a serum environment - modelling that in the subgingival pocket.

Methods

Growth and proteolytic activity of three *P. gingivalis* strains in nutrient-rich broth or a serum environment were assessed using A_{600} and a fluorescent protease substrate, respectively. Adherence of *P. gingivalis* strains to serum-coated surfaces was studied with confocal microscopy and 2D-gel electrophoresis of bacterial supernatants used to investigate extracellular proteins. A model multi-species sub-gingival community containing *Fusobacterium nucleatum, Streptococcus constellatus*, *Parvimonas micra* with wild type or isogenic mutants was then created and growth and proteolytic activity in serum assessed as above. Community composition over time was monitored using culture techniques and qPCR.

Results

The *P. gingivalis* strains showed different growth rates in nutrient-rich broth related to the level of proteolytic activity (largely gingipains) in the cultures. Despite being able to adhere to serum-coated surfaces, none of the strains was able to grow alone in a

serum environment. In the subgingival consortium however, all the included species were able to grow in the serum environment and the community adopted a proteolytic phenotype. Inclusion of *P. gingivalis* strains lacking gingipains in the consortium revealed that the ability of the community to grow was largely due to Rgp gingipain.

Conclusions

In the multi-species consortium, growth was facilitated by the wild-type and Rgp-expressing strains of *P. gingivalis,* suggesting that Rgp is involved in delivery of nutrients to the whole community through degradation of complex serum substrates. Whereas they are constitutively expressed by *P. gingivalis* in nutrient-rich broth, gingipain expression in the model periodontal pocket environment (serum) appears to be orchestrated through signaling to *P. gingivalis* from other members of the community, a phenomenon which can then promote growth of the whole community.

Keywords: Microbial community, Periodontitis, Dysbiosis, Virulence, Proteolytic activity

Background

The human oral cavity is a highly complex ecosystem in which the tooth- and soft-tissue surfaces offer distinct ecological niches for microbial colonization. Reflecting this habitat diversity, the oral microbiome has been shown to comprise at least 600 different bacterial species [1], of which up to 300 can be found in a single individual [2]. In health, microbial communities exist in a homeostatic balance with the host that contributes to ecosystem stability and provides resistance to colonization by exogenous pathogens. In periodontitis, however, the development of periodontal pockets as a result of breakdown of the bone and soft-tissues supporting the teeth, creates a new subgingival niche that promotes growth of bacterial species suited to the environment. When the adjacent gingival soft-tissues are inflamed, the flow of serum-like transudate [gingival cervical fluid (GCF)] into the pocket increases and under the influence of this environmental perturbation, homeostasis in the subgingival microbial community can be disturbed giving rise to dysbiosis that predisposes the site to disease [3]. Dysbiotic subgingival communities are characterized by a relative increase in abundance of anaerobic, Gram-negative bacterial species that can exploit protein-rich GCF as a nutrient source, promoting development of a proteolytic community phenotype. While around 60% of individuals are estimated to have periodontal pockets at occasional sites in the dentition, only around 7% will develop such severe disease that they risk losing teeth [4,5]. Currently, the lack of robust tools to identify the individuals with a high degree of risk for tooth loss means that even people who may not develop severe disease undergo intensive treatment, placing a significant burden on healthcare budgets in the developed world.

The subgingival microbiota in the periodontal pocket comprises thin, densely packed biofilms associated with the tooth and epithelial lining, and a community of loosely

89 attached “planktonic cells” in the bulk fluid [6]. In GCF, survival most likely depends on
90 co-operation between different members of the microbial community since a wide
91 range of different catabolic enzymes is required to exploit the complex proteins and
92 glycoproteins as a nutrient source [7]. In addition to metabolic cross-talk, the
93 microorganisms participate in synergistic and antagonistic interactions which
94 determine the overall properties and contribute to the resilience of the microbial
95 community in the face of environmental fluctuations [8,9]. Many studies have focused
96 on the composition of sub-gingival microbial communities in periodontitis and
97 comparison between healthy subjects and patients with periodontitis has revealed a
98 strong association between Gram-negative, proteolytic species such as *Treponema*
99 *denticola*, *Tannerella forsythia* and *Porphyromonas gingivalis* (termed red-complex
100 organisms) as well as a less stringent association between *Prevotella spp*,
101 *Fusobacterium spp* and *Parvimonas micra* (termed orange-complex organisms) and
102 increasing depth of the periodontal pocket [10]. Involvement of these organisms is
103 supported by 16S *r*RNA sequencing studies where *Treponema spp*, *T. forsythia*, *P.*
104 *gingivalis*, *P. micra* and *Peptostreptococcus spp* showed a higher prevalence and
105 abundance in patients with periodontitis than in healthy individuals [11].
106 The role of periodontitis-associated microorganisms in dysbiosis has largely focused
107 on *P. gingivalis,* revealing this organism to be capable of compromising the host
108 immune response through impairment of leukocyte activity and cytokine paralysis. This
109 has led to the proposal of *P. gingivalis* as a keystone pathogen in the disease [12,13].
110 Although the primary role of the proteolytic enzymes, arginine- and lysine-specific
111 cysteine proteases or gingipains (Rgp and Kgp) for the organism is most likely the
112 generation of nutrients from protein substrates, they are regarded as important factors
113 in *P. gingivalis* virulence. However, while inoculation of specific pathogen-free mice

with *P. gingivalis* induces significant periodontal bone loss, this is not the case in germ-free animals, indicating that the capacity of this organism to cause disease is dependent upon the presence of other bacteria [14]. This could explain why the levels of *e.g*. gingipains vary between periodontitis patients and suggests that interactions between bacteria in the microbial community in the periodontal pocket could conspire to influence the virulence of *P. gingivalis* [15].

In this study, we characterize the virulence properties of *P. gingivalis* strains alone and as part of a subgingival community in a serum environment - modelling that in the subgingival pocket. We show that polymicrobial interactions play a central role in the development of a community-wide virulent phenotype (proteolytic activity) as well as production of gingipains by *P. gingivalis*.

Methods

Bacterial strains

The *P. gingivalis* strains used were ATCC 53978 (W50) [16] as well as two clinical strains (33F and SUB1) freshly isolated from sub-gingival pocket samples of patients with periodontal disease [>2 sites with inflammation (bleeding on probing) and alveolar bone loss exceeding 1/3 root length] [17]. After recovery on Brucella agar, clinical strains were identified as *P. gingivalis* through morphology (glossy black-pigmented colonies containing small Gram-negative coccoid rods) and physiological testing (positive for trypsin and indole production but negative for fluorescence and β-galactosidase activity). Isogenic mutants of W50 (E8 –expressing only Kgp and K1A –expressing only Rgp) were used to study the role of gingipains in growth of the multi-species communities. The *Parvimonas micra* strain (ECE) was recovered as small white colonies on Brucella agar from a sub-gingival pocket sample of a patient with

periodontal disease (see above) while *F. nucleatum* (BK:0) was recovered from sub-gingival plaque of a healthy individual. The identities of the clinical strains of *P. gingivalis*, *P. micra* and *F. nucleatum* were confirmed by 16S *r*RNA gene sequencing. *Streptococcus constellatus* was a reference strain (NCTC 10714). All strains were stored at –70°C in skim milk (Oxoid) and routinely cultured on Brucella agar at 37°C under anaerobic conditions (10% H_2, 5% CO_2 in N_2).

Growth of individual strains

The *P. gingivalis* strains were grown in pre-reduced nutrient-rich broth [Bacto™ brain-heart infusion supplemented with 500µg/ml L-cysteine (BHI)] for 4 days under anaerobic conditions with equal numbers of bacteria [absorbance at 600nm (A_{600}) = 0.1] in the starter cultures. Aliquots were removed at intervals and bacterial growth assessed as increase in A_{600}. The capacity of the *P. gingivalis* strains as well as *P. micra*, *F. nucleatum* and *S. constellatus* to grow in a serum environment was evaluated by inoculating them into heat-inactivated equine serum (Håtunalab, AB, Bro Sweden) diluted 1:5 with PBS to give A_{600} = 0.1 and maintaining under anaerobic conditions. Aliquots were removed at intervals and bacterial growth assessed as above.

Measurement of proteolytic activity

Proteolytic activity was determined by mixing 10µl aliquots of the bacterial suspensions with 100µl FITC-conjugated gelatin (1mg/ml DQ™ gelatin, Molecular probes) in a 96-well plate and incubating at 37°C. Fluorescence was measured at 1 min intervals using a BMG Clariostar plate reader [excitation 485nm, emission 530 nm). Values for the negative control (BHI broth or serum alone) were subtracted and the final values expressed as relative fluorescence units per min (RFU/min). To assess cell-associated proteolytic activity, a 10µl aliquot of bacterial suspension was incubated with 1µl FITC-

conjugated gelatin for 30 min at 37°C and then viewed using a Nikon Eclipse TE2000 inverted confocal scanning laser microscope (CSLM) (Nikon Corp., Tokyo, Japan). Images were acquired with an oil immersion objective (x60) and illumination provided by an Ar laser (488 nm excitation).

Zymography

Cell suspensions containing approximately 20µg of protein were run at 125V, 4°C on Novex 10% Zymogram plus gels containing gelatin. The running buffer [25mM Tris, 192mM glycine, buffer pH 8.3 containing 0.5% SDS] was kept at 4°C. Gels were renatured by replacement of SDS with 25% Triton X-100 using Novex Zymogram Renaturing buffer (4°C for 30 minutes) so that proteins were shifted from non-catalytic to catalytic conditions. Gels were equilibrated with Zymogram Developing Buffer containing 2mM L-cysteine for 30 minutes at 4°C. Fresh developing buffer containing 2mM L-cysteine was then added and the gel incubated at 37°C for 2 hours. Finally, gels were stained with colloidal Coomassie brilliant blue G overnight and excess stain removed in 25% ethanol for 1 hour at room temperature. All gels and reagents were from Invitrogen. Preparations of Kgp (GingisKHAN®) and Rgp (Gingis REX®) for purchased from Genovis AB, Sweden were used for comparison.

Two-dimensional gel electrophoresis

Late log-phase cultures of the *P. gingivalis* strains were centrifuged (3000*g*, 15 min, 4°C), and the supernatants filtered to remove bacterial cells. Filtrates were mixed 1:10 with ice-cold TCA and maintained overnight on ice. Precipitated extracellular proteins were harvested by centrifugation (16 000*g*, 30 min, 4°C) and the pellets re-suspended in ice-cold acetone, sonicated (3 x 10s) and subjected to a second round of centrifugation. After removal of the acetone, the pellet was air-dried, re-suspended in

1ml rehydration buffer (8 M urea, 2% CHAPS, 10 mM DTT, 2% IPG buffer; GE Healthcare Life Sciences) and stored at -20 °C until use. The protein concentration was determined using a 2D-Quant kit (GE Healthcare Life Sciences). Volumes corresponding to 20 μg protein were subjected to 2D-gel electrophoresis essentially as described previously [18]. Isoelectric focusing was carried out on 18-cm pH 4-7 linear immobilized pharmalyte gradient strips followed by gel electrophoresis on 10% polyacrylamide gels. Gels were stained with colloidal Coomassie brilliant blue G. The most abundant proteins were excised manually and subjected to LC-MS/MS as described previously [32]. Mass lists were created automatically and used as the input for Mascot MS/MS Ions searches of the NCBInr database using the Matrix Science web server. Parameters were set to 0.5 Da peptide mass tolerance, methionine oxidation and carboxyamidomethyl cysteine modification.

Adherence assay

Mini flow-cells (IbiTreat μ-slide VI) were coated overnight at room temperature with serum diluted 1:5 in PBS (0.15M NaCl, 10mM NaH_2PO_4 buffer, pH 7.4) and the channels rinsed twice with pre-reduced PBS before use. Suspensions of the *P. gingivalis* strains were prepared by harvesting colonies from Brucella agar plates and dispersing them in pre-reduced PBS to give OD_{600} = 0.4. Aliquots were added to the channels and the slides incubated anaerobically for 2h. After rinsing 3 times with pre-reduced PBS, adherent bacteria were stained with *Bac*Light Live/Dead stain and viewed with a CSLM as described above. All experiments were carried out in triplicate and data analyzed using GraphPad Prism Software. Bacterial surface coverage on the coated surfaces was compared with that on uncoated ones using a two-tailed Mann Whitney U-test and p values less than 5% were regarded as significant.

Formation of polymicrobial communities

Suspensions of each individual bacterium were formed by taking colonies from blood agar and suspending them in serum (1:5 in PBS) to give A_{600} = 0.1. Three different polymicrobial communities were then created by mixing equal volumes of each bacterial suspension (*P. micra*, *S. constellatus* and *F. nucleatum*) with *P. gingivalis* strain W50, E8 or K1A. Cultures were maintained under anaerobic conditions for up to 9 days and aliquots removed at intervals. The A_{600} and general proteolytic activity (as described above) were monitored. An aliquot was also plated onto Brucella agar and the relative numbers of the different bacteria in the consortium enumerated after identification based on colony morphology [*P. gingivalis*; glossy black-pigmented colonies, *P. micra*; small (1-2mm) round, peaked colonies showing anaerobic growth but no growth in CO_2, *S. constellatus*; large (5-10mm) white colonies containing cocci in chains and *F. nucleatum*; large (6mm), low convex white/grey glistening colonies containing slender rods with pointed ends].

Real-time quantitative PCR (qPCR)

For qPCR analysis of composition in the subgingival consortia, DNA was extracted using a QIAamp UCP Pathogen mini-kit (Qiagen) according to the manufacturer's instructions. A lysozyme treatment step (20 mg/ml lysozyme in 20 mM Tris pH 8.0, 2 mM EDTA, 1,2 % Triton X-100), 37 °C for 1 h) and lysis using 0.1mm glass beads (5 x 5 min x 50 Hz in a Tissue-Lyser LT (Qiagen)] followed by incubation with proteinase K (20 min, 56 °C) were used to ensure adequate extraction from Gram-positive cells. Primer sequences for the 16S *r*RNA genes were: *P. gingivalis* (f:5'-TGTAGATGACTGATGGTGAAAACC-3', r:5'-ACGTCATCCCCACCTTCCTC-3') [19], *P. micra* (f:5'-TCGAACGTGATTTTTGTGGAAA-3', r:5'-GGTAGGTTGCTCACGTGTT ACTCA-3') [20], *F. nucleatum* (f:5'-CGCAGAAGGTGAAAGTCCTG TAT-3', r:5'-TGGTCCTCACTGATTCACACAGA-3') [21] and *S. constellatus* (f:5'-AGATG

GACCTGCGTTGT-3', r:5'-TGCCTCCCGTAGGAGTCT-3') [22]. Total DNA template used was 4-28ng in each triplicate reaction and negative controls (no DNA template) were prepared alongside the experimental samples to normalize for background signal in the amplification step. Estimates of cell number were made against standards prepared from 10-fold serial dilutions of each bacterium (ranging between 10-18 ng and 1-1.8 pg/µl). Quantifications were based on the following estimated 16S rRNA gene copy numbers and amounts of chromosomal DNA in each cell (*P. gingivalis*: 4 copies, 2.5fg, P*. micra*: 3 copies, 1.9fg, *F. nucleatum*: 5 copies, 2.3fg and *S. constellatus*: 4 copies, 2.4fg) obtained from the Ribosomal RNA Operon Copy Number Database (https://rrndb.umms.med.umich.edu/search/) and NCBI genome database (http://www.ncbi.nlm.nih.gov/sites/genome) respectively.

16S *r*RNA fluorescent *in situ* hybridization (FISH)

Aliquots from the polymicrobial communities were placed in ibiTreat mini flow-cells and fixed with 4% paraformaldehyde in PBS overnight at 4°C. FISH was then performed largely as described previously [23]. Briefly, cells were permeabilized using lysozyme (10 mg/mL), washed with ultra-pure water and dehydrated with 50%, 80% and 99% ethanol for 3 min each. Finally, 30 mL of hybridization buffer (0.9 M NaCl, 20 mM Tris-HCl buffer, pH 7.5, with 0.01% sodium dodecyl sulfate and 25% formamide) containing 3.3pmol/µL of the oligonucleotide probes was added and hybridization performed at 48ºC for 90 min in a humid chamber. Probes were synthesized by biomers.net Gmbh (Ulm/Donau, Germany). *P. gingivalis* was identified using the POGI probe (CAATACTCGTATCGCCCGTTATTC) [24] fluorescently labeled with Atto-565 (red), *F. nucleatum* was identified using the FUSall307 probe (TCAGTCCCCTTG GCCG) [25] labeled with Atto-488 (green), *P. micra* was identified using the PAMIC1435 probe (TGCGGTTAGATCGGCGGC) [26] double-labeled with Atto-390 (blue) and *S.*

constellatus was identified using the STR405 probe (TAGCCGTCCCTTTCTGGT) [27] double-labeled with cyanine3 and ATTO-488 yielding yellow fluorescence.

Results

P. gingivalis strains show different rates of growth and proteolytic activities

Initially, growth of *P. gingivalis* strains (W50, 33F or SUB1) was compared under anaerobic conditions in nutrient-rich broth for 5 days. Their growth rates differed significantly, with W50 and 33F showing rapid and strong growth over the first 48 hours while SUB1 showed low initial growth which continued to increase steadily over time (Figure 1a). Since extracellular proteases are important in the generation of nutrients for cell growth, we investigated whether growth rate was related to the proteolytic activity in the cultures. On days 1 and 3, strain 33F demonstrated a higher level of proteolytic activity than W50, while SUB1 showed a lower level (Figure 1b), indicating that the relative level of proteolytic activity corresponded well to the observed growth profile for each strain. Zymography of culture supernatants demonstrated a similar pattern for the three strains, with 2 prominent clear areas; one at a high-M*r* (>76 kDa) and a second in the region below 60 kDa (Figure 1c). Comparison with commercial preparations of Kgp and Rgp revealed the high and low-M*r* bands to coincide with Kgp/RgpA and RgpB, respectively. Although only semi-quantitative, the gels appeared to indicate that Kgp/RgpA activity was similar for all strains whereas the RgpB band was most intense for strain 33F and least intense for SUB1.

Identification of extracellular proteases of *P. gingivalis* strains

To further investigate the proteins associated with activity in the zymograms, supernatants from the *P. gingivalis* cultures were subjected to 2D-PAGE, stained with Coomassie blue and the major spots identified using LC-MS/MS. The protein profiles

of the three strains shared some common features in the high-M*r* range (>76 kDa) but more variation was seen in the spots present at lower M*r* (Figure 2). Mapping of the peptide sequences from the most intense spots to *P. gingivalis* genomes revealed the presence of six major proteins, which could be clustered into different functional groups (Table 1). Strain 33F showed multiple spots identified as fimbrillin as well as the outer membrane protein Tap A, which was also highly expressed in SUB1. Neither of these were seen in W50. Peptidyl arginine deiminase was also present in strain 33F but not SUB1 or W50. All three strains gave rise to multiple spots corresponding to known *P. gingivalis* proteases, predominantly various forms of Rgp and Kgp. Due to the high degree of sequence homology between these two molecules, it was not always possible to differentiate between them with certainty and spots are therefore annotated as gingipain. The most prominent spots in the high-M*r* range (around 200kDa) corresponded to full-length versions of gingipains. Additional spots at lower molecular weights were identified as gingipain fragments. Two other proteases; a member of the M16 protease family and a conserved hypothetical protein with a zinc carboxypeptidase domain, were identified in one spot in 33F and SUB1 respectively. Taken together, these data suggest that gingipains most likely account for most of the extracellular proteolytic activity in all three *P. gingivalis* strains.

Survival of *P. gingivalis* alone in a serum environment

The ability to attach to a surface is an important virulence factor for *P. gingivalis* in colonizing the periodontal pocket. Therefore, the different *P. gingivalis* strains were tested for their ability to form biofilms on serum-coated surfaces (Figure 3a). CSLM revealed significantly higher coverage (1.75-4-fold increase) on the serum-coated surface for all strains compared to an uncoated surface ($p<0.01$). The absolute levels

of coverage on the serum-coated surfaces differed with W50 showing a significantly higher capacity for adherence than the clinical isolates (SUB1 and 33F). However, all strains formed large aggregates in solution suggesting that they interact with proteins in serum (data not shown). To determine whether serum could support growth of the *P. gingivalis* strains, growth of W50, SUB1 and 33F was monitored over 5 days (Figure 3b). This revealed that none of the strains was able to grow and that this lack of growth was associated with the absence of proteolytic activity in the cultures (Figure 3c).

Growth of a multi-species community containing *P. gingivalis* in a serum environment

The capacity for growth and survival in the serum environment was then tested when *P. gingivalis* was present as part of a multi-species community containing three other sub-gingival colonizers: *F. nucleatum*, *P. micra* and *S. constellatus*. In contrast to mono-species cultures, steady growth of multi-species communities containing *P. gingivalis* strain W50 was seen over time (Figure 4a). To ensure that this was not due to the ability of one of the other species to exploit the serum as a growth medium, growth curves were also constructed for *F. nucleatum*, *P. micra* and *S. constellatus* as mono-species cultures. This revealed that none of these bacteria were able to grow alone in serum (data not shown). 16S *r*RNA-FISH revealed the presence of all four bacteria in the multi-species community after 2 days and *S. constellatus* appeared to be associated with *F. nucleatum* while *P. micra* formed clusters with *P. gingivalis* (Figure 4b). When W50 was replaced in the consortium with the isogenic mutant expressing Rgp only (K1A), growth was facilitated whereas no consortium growth was seen when the Kgp expressing mutant was included (Figure 4a).

A more detailed compositional analysis of the communities containing *P. gingivalis* strains W50, K1A and E8 was then undertaken using culture techniques (Figure 4c). For the consortium with W50 at time 0, the bacterial count was around 10^8 cells/ml, (corresponding to OD_{600} = 0.1), with an approximately equal distribution of the four species. After 2 days, the total count had risen to approximately 10^{10} cells/ml (corresponding to OD_{600} = 0.6). All the species in the consortium exhibited growth with *P. gingivalis*, *P. micra* and *F. nucleatum* increasing one hundred-fold and *S. constellatus* showing a ten-fold increase in CFU/ml. A similar pattern was seen for the consortium containing K1A. In contrast, the consortium containing E8 showed no growth over 2 days (no change in OD_{600}) and the number of living bacteria decreased from around 10^8 to 10^7 cells/ml. For the W50 and K1A-containing consortia that showed growth in serum, the species composition obtained by culturing was confirmed using qPCR (Figure 4d).

Development of proteolytic activity in the multi-species community

Growth of the consortium containing W50 and K1A but not E8 strongly suggests a role for Rgp in facilitating growth in serum. We therefore investigated development of proteolytic activity in the multi-species community containing *P. gingivalis* strain W50 and the isogenic mutant strains over time. This showed that the total activity increased significantly over 4 days in the communities containing W50 and K1A, but not E8 (Figure 5a). Zymogram analysis revealed bands associated with the positions of Kgp/RgpA and RgpB in the W50-containing consortium (Figure 5b). Similar bands were seen in the consortium containing the Rgp-expressing strain, but not that expressing Kgp, suggesting that the activity in the W50 consortium can mainly be attributed to Rgp. Application of the fluorescent general protease substrate to bacteria

in the multi-species community revealed that the strongest activity was associated with clumps of cells (Figure 5c). 16S *r*RNA-FISH revealed these clusters to correspond to co-aggregates of *P. gingivalis* and *P. micra* (Figure 5c, insert). Chains of *S. constellatus* were unstained, confirming that they did not express proteolytic activity on the cell surface, however some weak staining was seen on long spindle-shaped *F. nucleatum* cells (Figure 5c). However, *F. nucleatum*, *S. constellatus* and *P. micra* did not show any proteolytic activity alone in either nutrient-rich broth or serum as shown by zymography (data not shown). Together, these data suggest that Rgp from *P. gingivalis* is the major component of the overall proteolytic phenotype of the community and is essential for growth of all community members.

Discussion

It is widely acknowledged that periodontitis is associated with a substantial enrichment of anaerobic and proteolytic bacteria in sub-gingival microbial communities. The driving force for this dysbiosis is thought to be increased flow of protein-rich GCF, but the underlying mechanisms are not fully understood. We therefore investigated development of a proteolyic phenotype in a multi-species community, a factor that we propose is essential to the initiation and progression of periodontitis. In this simplified model, serum was used to model GCF, together with a consortium comprising four sub-gingival bacterial species: *P. gingivalis* belonging to the red complex and *P. micra, F. nucleatum* and *S. constellatus* belonging to the orange complex as defined by Socransky *et al*. [10]. Recently, studies have shown that all these bacteria are part of the core microbiome in periodontitis [11].

Prior to studies in the community, the virulence properties (ability to bind to serum-coated surfaces, growth and proteolytic activity) of three *P. gingivalis* strains were

386 investigated. Serum increased surface coverage of all strains, suggesting that proteins
387 in the gingival exudate enhance adherence of *P. gingivalis,* thus promoting colonization
388 of the periodontal pocket. Proteomic analysis revealed multiple extracellular isoforms
389 of fimbrillin in strain 33F, consistent with expression of FimA fimbriae, whereas no
390 fimbrillin was seen in strains SUB1 or W50, in keeping with reports that W50 is sparsely
391 fimbriated [28]. Strain 33F showed the lowest absolute level of binding and the lack of
392 a strong relationship between the presence of fimbrillin and adherence suggests that
393 FimA is not critical for binding to surface-associated serum proteins. This is in
394 agreement with a previous study showing that *P gingivalis* fimbriae do not bind to
395 serum albumin [29] although FimA fimbriae are known to be important for binding of *P.*
396 *gingivalis* to other bacteria such as *Streptococcus oralis* [30].
397 Consistent with previous data [31], the growth rates in nutrient-rich broth differed
398 between the *P. gingivalis* strains and this was clearly related to the level of proteolytic
399 activity in the cultures. Zymography revealed the secreted proteolytic activity to be
400 present as 2 major bands consistent with the predicted positions of RgpA/Kgp and
401 RgpB respectively [32]. Characterization of extracellular proteins confirmed that
402 gingipains, secreted via the type IX secretion system [33], were the predominant
403 proteases from all the wild-type *P. gingivalis* strains. As well as the high-M_r forms of
404 Rgp and Kgp, a large number of lower M_r gingipain fragments were identified. The
405 broad bands seen on the zymogram gels appear to indicate that many were
406 proteolytically active. The clinical strains (33F and SUB1), produced two
407 metalloproteinases: a zinc-carboxypeptidase and an M16-family protease, whose
408 functions are currently unknown, as well as an outer membrane protein; Tap A (61KDa
409 antigen) belonging to the CTD protein family, thought to be involved in *P. gingivalis*
410 virulence [34], and peptidylarginine deiminase, involved in protein citrullination. None

411 of these was found in W50. Overall, the extracellular proteomes agree with those seen
412 in other studies and, in keeping with previous work, there are variations between the
413 different strains which may impact on their virulence as well as their ability to survive
414 in multi-species communities [35].

415 The *P. gingivalis* strains used in this study were unable to grow as mono-species
416 cultures in serum. Previous investigations of the ability of *P. gingivalis* to exploit serum
417 proteins show conflicting results, with some suggesting that *e.g.* human or bovine
418 serum albumin can support growth and others suggesting that it does not [36-38].
419 However, importantly, all these studies used defined basal media supplemented with
420 serum proteins rather than serum alone. Introduction of *P. gingivalis* into the multi-
421 species consortium containing *S. constellatus*, *P. micra* and *F. nucleatum* led to steady
422 growth. Community composition remained stable over time as shown using culturing
423 techniques and qPCR, indicating that all four species contributed to community growth.
424 This suggests that coordinated degradation, through expression of the required
425 repertoire of enzymes allowed the community to exploit the complex serum proteins
426 and glycoproteins. These could not be utilized by any of the individual species alone.
427 Similar phenomena have been described previously, where almost complete
428 degradation of serum proteins was achieved by a plaque-derived consortium selected
429 through growth in serum [39,40] and a consortium of plaque bacteria was required to
430 degrade complex salivary glycoproteins [41]. In parallel with growth, the overall level
431 of proteolytic activity in the community increased. The role of gingipains in community
432 growth was investigated by replacing W50 with the isogenic mutant strains; K1A
433 expressing only Rgp or E8 expressing only Kgp. In the presence of K1A, culturing and
434 qPCR revealed growth of all the community species, whereas no growth was seen in
435 the community containing E8, suggesting that Rgp from *P. gingivalis* plays a central

role in facilitating growth and maintaining diversity of the whole community. This was confirmed by zymography which revealed a prominent band corresponding to RgpB in the consortia containing W50 and K1A, which was absent in the E8-containing consortium. Microscopic examination of the consortium revealed the strongest proteolytic activity to be associated with clusters of bacteria corresponding to *P. gingivalis* and *P. micra*. In addition, some activity was associated with long, spindle-shaped cells of *F. nucleatum*, but it was not possible to determine whether this was due to expression of serine proteases known to be produced by these species [42,43] or, for instance, sequestration of gingipains onto the *F. nucleatum* cell surface. Thus, we have shown that growth of all species in the multi-species community appears to be dependent on RgpB from *P. gingivalis*. While W50 expressed high levels of Kgp/RgpA and RgpB in nutrient-rich broth, this wild type strain showed no growth or proteolytic activity in single-species culture in serum suggesting that gingipain expression in this environment required the presence of other members of the consortium. Gingipain expression has been proposed to be regulated by environmental cues and nutritional status [32] and we have shown previously that Rgp expression increases significantly in multi-species communities in response to heat-sensitive factors from *P. micra* [44]. This could explain why *P. gingivalis* requires the presence of the commensal microflora for the development of periodontitis in animal models [14] as well as the observation that *P. gingivalis* is often isolated from apical periodontal abscesses as part of a consortium together with *Fusobacterium* and *P. micra* [45].

Conclusions

P. gingivalis strains grow at different rates and show different levels of proteolytic activity in nutrient-rich broth, but despite being able to attach to serum-coated surfaces, none of the strains used here was able to survive alone in a serum environment. In a multi-species consortium, community growth was facilitated in the presence of wild-type and an Rgp-expressing strain of *P. gingivalis* suggesting that Rgp may be involved in delivery of nutrients through degradation of complex serum substrates. Whereas they are constitutively expressed by *P. gingivalis* in nutrient-rich broth, gingipain expression in an environment modelling the periodontal pocket appears to be orchestrated through signaling to *P. gingivalis* from other members of the community. This phenomenon appears to facilitate growth of the whole community thus likely contributing to the maintenance of microbial diversity within the periodontal pocket.

Declarations

Ethics approval and consent to participate

Not applicable

Consent for publication

Not applicable

Availability of data and materials

The datasets used and/or analysed during the current study are available from the corresponding author on reasonable request

Competing interests

The authors declare that they have no competing interests

Funding

This study was funded by The Foresight Research Programme at Malmö University, The Swedish Research Council, The Knowledge Foundation, Sweden and Odontologisk Forskning Region Skåne.

Authors' contributions

JD and GS designed the project, TK, JD, JN, ZP, GS, TB, HK and BK performed the experiments and analysed the data. All authors contributed to and approved the manuscript.

Acknowledgements

We gratefully acknowledge excellent technical assistance from Agnethe Henriksson and Madeleine Blomqvist.

References

1. Dewhirst FE, Chen T, Izard J, Paster BJ, Tanner AC, Yu WH, Lakshmanan A, Wade WG. The human oral microbiome. J Bacteriol. 2010;192:5002-17.

2. Kilian M, Chapple IL, Hannig M, Marsh PD, Meuric V, Pedersen AM, Tonetti MS, Wade WG, Zaura E. The oral microbiome – an update for oral health professionals. Br Dent J. 2016;18:657-66.

3. Naginyte M, Do T, Meade J, Devine DA, Marsh PD. Enrichment of periodontal pathogens from the biofilms of healthy adults. Sci Rep. 2019;9(1):5491.

4. Swedish Council on Health Technology Assessment in Health Care (SBU). Chronic periodontitis – prevention, diagnosis and treatment. Stockholm: 2004. Report no 169 (in Swedish). Summary and conclusions in English.

5. Kassebaum NJ. Bernabé E, Dahiya M, Bhandari B, Murray CJ, Marcenes W. Global, Regional, and National Prevalence, Incidence, and Disability-Adjusted Life Years for Oral Conditions for 195 Countries, 1990-2015: A Systematic Analysis for the Global Burden of Diseases, Injuries, and Risk Factors. J Dent Res. 2017;96:380-87.

6. Socransky SS, Haffajee AD. Dental biofilms: difficult therapeutic targets. Periodontology *2000* 2002;28:12-55.

7. Marsh PD, Zaura E. Dental biofilm: ecological interactions in health and disease. J Clin Periodontol. 2017;44 Suppl 18:12-22.

8. Rosier TB, Marsh PD, Mira A. Resilience of the oral microbiota in health: mechanisms that prevent dysbiosis. J Dent Res. 2018;97:371-80.

9. Jakubovics NS. Intermicrobial interactions as a driver for community composition and stratification of oral biofilms. J Mol Biol. 2015;427:3662-72.

10. Socransky SS, Haffajee AD, Cugini MA, Smith C, Kent RL. Microbial complexes in subgingival plaque. J Clin Periodontol. 1998;25:134-44.

11. Abusleme L, Dupuy AK, Dutzan N, Silva N, Burleson JA, Strausbaugh LD, Gamonal J, Diaz PI. The subgingival microbiome in health and periodontitis and its relationship with community biomass and inflammation. ISME J. 2017;7:1016-25.

12. Lamont R, Koo H, Hagishengallis G. The oral microbiota: dynamic communities and host interactions. Nat Rev Microbiol. 2018;16:745-59.

524 13. Hajishengallis G, Darveau RP, Curtis MA. The keystone-pathogen hypothesis. Nat
525 Rev Microbiol. 2012;10:717-25.

526 14. Hajishengallis G, Liang S, Payne MA, Hashim A, Jotwani R, Eskan MA, McIntosh
527 ML, Alsam A, Kirkwood KL, Lambris JD, Darveau RP, Curtis MA. Low-abundance
528 biofilm species orchestrates inflammatory periodontal disease through the commensal
529 microbiota and complement. Cell Host Microbe. 2011;17:497-506.

530 15. Zenobia C, Hajishengallis G. *Porphyromonas gingivalis* virulence factors involved
531 in subversion of leukocytes and microbial dysbiosis. Virulence. 2015;6:236-43.

532 16. O'Brien-Simpson NM, Paolini RA, Hoffmann B, Slakeski N, Dashper SG, Reynolds
533 EC. Role of RgpA, RgpB, and Kgp proteinases in virulence of *Porphyromonas*
534 *gingivalis* W50 in a murine lesion model. Infect Immun. 2001;69:7527-34.

535 17. Lang NP, Tonetti. MS. Periodontal risk assessment (PRA) for patients in supportive
536 periodontal therapy (SPT). Oral Health Prev Dent. 2003;1:7-16.

537 18. Davies JR, Svensäter G, Herzberg MC. Identification of novel LPXTG-linked
538 surface proteins from *Streptococcus gordonii.* Microbiology. 2009;155:1977-88.

539 19. Kuboniwa M, Amano A, Kimura KR, Sekine S, Kato S, Yamamoto Y, Okahashi N,
540 Iida T, Shizukuishi S. Quantitative detection of periodontal pathogens using real-time
541 polymerase chain reaction with TaqMan probes. Oral Microbiol Immunol. 2004;19:
542 168-76.

543 20. Schwarz F, Becker K, Rahn S, Hegewald A, Pfeffer K, Henrich B. Real-time PCR
544 analysis of fungal organisms and bacterial species at peri-implantitis sites. Int J Implant
545 Dent. 2015;1:9.

546 21. Suzuki N, Yoshida A, Saito T, Kawada M, Nakano Y. Quantitative microbiological
547 study of subgingival plaque by real-time PCR shows correlation between levels of
548 *Tannerella forsythensis* and *Fusobacterium spp*. *J Clin Microbiol.* 2004;42:2255-57.

549 22. Dalwai F, Spratt DA, Pratten J. Use of quantitative PCR and culture methods to
550 characterize ecological flux in bacterial biofilms. *J Clin Microbiol.* 2007;45:3072–76.

551 23. Kinnby B, Chávez de Paz LE. Plasminogen coating increases initial adhesion of
552 oral bacteria *in vitro*. Microb Pathogen. 2016;**100**:10-16 .

553 24. Sunde PT, Olsen I, Göbel UB, Theegarten D, Winter S, Debelian GJ, Tronstad L,
554 Moter A.Fluorescence *in situ* hybridization (FISH) for direct visualization of bacteria in
555 periapical lesions of asymptomatic root-filled teeth. Microbiology. (2003;149:1095-
556 1102.

557 25. Juretschko S, Fritsche T. Applications of fluorescence *in situ* hybridization in
558 diagnostic microbiology, (2011) pp 3-19. In: Persing, D., Tenover, F., Tang, Y., Nolte,
559 F., Hayden, R., van Belkum, A. (ed), Molecular Microbiology. ASM Press, Washington,
560 DC.

561 26. Wildeboer-Veloo ACM, Harmsen HJM, Welling GW, Degener JE. Development of
562 16S *r*RNA-based probes for the identification of Gram-positive anaerobic cocci isolated
563 from human clinical specimens. Clin Microbiol Infect. 2007;13:985–92.

564 27. Paster BJ, Bartoszyk IM, Dewhirst FE. Identification of oral streptococci using PCR-
565 based, reverse-capture, checkerboard hybridization. Methods Cell Sci. 1998;20:223-
566 31.

28. Handley PS, Tipler LS. An electron microscope survey of the surface structures and hydrophobicity of oral and non-oral species of the bacterial genus *Bacteroides.* Arch Oral Biol. 1986;31:325-35.

29. Sojar HT, Smith DF. *Porphyromonas gingivalis* fimbriae carbohydrate specificity assessment by glycomics. *FEMS Immunol Med Microbiol.* 2012;66:83-7.

30. Maeda K, Nagata H, Yamamoto Y, Tanaka M, Tanaka J, Minamino N, Shizukuishi S. Glyceraldehyde-3-phosphate dehydrogenase of *Streptococcus oralis* functions as a co-adhesin for *Porphyromonas gingivalis* major fimbriae. Infect Immun. 2004;72:1341-48.

31. Seers, CA, Mahmud SM, Huq NL, Cross KJ, Reynolds EC. *Porphyromonas gingivalis* laboratory strains and clinical isolates exhibit different distribution of cell surface and secreted gingipains. J Oral Microbiol. 2020;13:1-14.

32. Curtis MA, Aduse-Opoku J. Rangarajan M. Cysteine proteases of *Porphyromonas gingivalis*. Crit Rev Oral Biol Med*. 2001;*12:192-216.

33. Silva IL, Cascales. E. Molecular strategies underlying Porphyromonas gingivalis virulence. J Mol Biol. 2021;433:166836.

34. Kondo Y, Ohara N, Sato K, Yoshimura M, Yukitake H, Naito M, Fujiwara T, Nakayama K. Tetratricopeptide repeat protein-associated proteins contribute to the virulence of *Porphyromonas gingivalis*. Infect Immun. 2010;78:2846-56.

35. Stobernack T, Glasner C, Junker S, Gabarrini G, de Smit M, de Jong A, Otto A, Becher D, van Winkelhoff AJ, van Dijl JM. Extracellular proteome and citrullinome of the oral pathogen *Porphyromonas gingivalis*. J Proteome Res. 2016;15:4532-45.

589 36. Leduc A, Grenier D, Meyrand D. Comparative growth of *Porphyromonas gingivalis*
590 strains in a defined basal medium. Anaerobe. 1996;2:257-61.

591 37. Grenier D, Imbeault S, Plamondon P, Grenier G, Nakayama K, Mayrand D. Role
592 of gingipains in growth of *Porphyromonas gingivalis* in the presence of human serum
593 albumin. Infect Immun. 2001;69:5166-72.

594 38. Lui X, Sroka A, Potempa J, Genco CA. Coordinate expression of the
595 *Porphyromonas gingivalis* lysine-specific gingipain proteinase, Kgp, arginine-specific
596 gingipain proteinase, RgpA, and the heme/hemoglobin receptor, HmuR. Biol Chem.
597 2004;385:1049-57.

598 39. ter Steeg PF, Van der Hoeven JS, de Jong MH, van Munster PJ, Jansen MJ.
599 Enrichment of subgingival microflora on human serum leading to accumulation of
600 *Bacteroides* species, *Peptostreptococci* and *Fusobacteria*. Antonie Van Leeuwenhoek.
601 1987;53:261-72.

602 40. ter Steeg PF, Van der Hoeven JS. Growth stimulation of *Treponema denticola* by
603 periodontal microorganisms. Antonie Van Leeuwenhoek. 1980;57:63-70.

604 41. Wickström C, Herzberg MC, Beighton D, Svensäter G. Proteolytic degradation of
605 human salivary mucin MUC5B by dental biofilms. Microbiology. 2009;155:2866-72.

606 42. Doron, L. Coppenhagen-Glazer S, Ibrahim Y, Eini A, Naor R, Rosen G, Bachrach
607 G. Identification and characterization of fusolisin, the *Fusobacterium nucleatum*
608 autotransporter serine protease. PLoS One. 2014;9(10):e111329.

609 43. Grenier D, Bouclin R. Contribution of proteases and plasmin-acquired activity in
610 migration of *Peptostreptococcus micros* through a reconstituted basement membrane.
611 Oral Microbiol Immunol. 2006;**21**:319-25.

612 44. Neilands J, Davies JR, Bikker FJ, Svensäter G. *Parvimonas micra* stimulates
613 expression of gingipains from *Porphyromonas gingivalis* in multi-species communities.
614 Anaerobe. 2018;55:54-60.

615 45. Zehnder, M. & Belibesakis G. On the dynamics of root canal infections – what we
616 understand and what we don't. *Virulence* **6**, 216-222 https:// doi:
617 10.4161/21505594.2014.984567 (2015).

618

619 **Legends**

620

621 **Table 1.** The most abundant proteins in the exoproteome of different strains of *P.*
622 *gingivalis* identified using 2D-gel electrophoresis and MS/MS-LC mass spectroscopy.
623 Mass lists were used as the input for Mascot MS/MS Ions searches of the NCBInr
624 database using the Matrix Science web server.

625

626 **Figure 1. Growth and proteolytic activity of *P. gingivalis* strains in nutrient-rich**
627 **broth**

628 (a) Growth of strains [33F (▲), W50 (❍) and SUB1 (◆)] in BHI over time was assessed
629 as absorbance at 600nm and the graph shows mean ± sd of three independent
630 biological replicates. (b) Proteolytic activity over time as assessed using a FITC-
631 conjugated gelatin substrate and expressed as trypsin equivalent units (TEU). The
632 graph shows mean ± sd of the same three independent biological replicates in (a). (c)

633 Aliquots from the cultures on day 3 were subjected to zymography on gelatin-
634 containing gels stained with Coomassie brilliant blue. All samples were run on the
635 same gel and the image has not been subject to digital enhancement or bands
636 removed by cropping. The original image is available in Supplementary File 1.
637
638 **Figure 2. 2DE gels of extracellular proteins from *P. gingivalis* strains**
639 Supernatants from cultures of *P. gingivalis* strains W50, 33F and SUB1 were subjected
640 to 2D-PAGE and the gels stained with Coomassie brilliant blue. The major spots were
641 excised and proteins identified using LC-MS/MS. Protein identities are presented in
642 Table 1.
643
644 **Figure 3. Survival of *P. gingivalis* strains in a serum environment**
645 (a) Graphs showing coverage of *P. gingivalis* strains 33F, W50 and SUB1 on surfaces
646 in the presence (■) or absence (□) of a serum coating. The bars show the mean ± sd
647 of three independent biological replicates. Representative images show adherent
648 bacteria stained with Baclight Live/Dead stain. The bar represents 10μm. **p<0.01. (b)
649 Growth of *P. gingivalis* strains 33F (▲), W50 (❍) and SUB1 (◆) in serum, assessed
650 as absorbance at 600nm. (c) Graph showing proteolytic activity of *P. gingivalis* strains
651 W50 (❍), K1A (∆) or E8 (●) in serum. The graph shows mean ± sd of three
652 independent biological replicates.
653
654 **Figure 4. Growth and composition over time of multi-species communities**
655 **containing *P. gingivalis* strains W50, K1A or E8 in serum**
656 (a) Graph showing growth of multi-species communities containing *P. gingivalis* strain
657 W50 (❍), K1A (∆) or E8 (●) in serum, assessed as absorbance at 600nm (mean ± sd

of three independent biological replicates). (b) A representative confocal FISH image showing composition of the W50-containing consortium after 2 days [*P. gingivalis* (red), *F. nucleatum* (green), *P. micra* (blue) and *S. constellatus* (yellow)]. The bar represents 10μm. Composition of multi-species communities containing *P. gingivalis* strains W50, K1A or E8 on day 0 and day 2 assessed using (c) growth on blood agar or (d) qPCR [*P. gingivalis* (red), *F. nucleatum* (green), *P. micra* (blue) and *S. constellatus* (yellow)]. Numbers represent mean ± sd of three independent replicates.

Figure 5. Proteolytic activity in multi-species communities containing *P. gingivalis* strains W50, K1A or E8 in serum

(a) Graph showing proteolytic activity of the multi-species communities containing *P. gingivalis* strains W50 (❍), K1A (∆) or E8 (●) in serum. The graph shows mean ± sd of three independent biological replicates. (b) Aliquots (2μl) from the cultures on day 0 and day 2 were subjected to zymography on gelatin-containing gels stained with Coomassie brilliant blue. All samples were run on the same gel and the image has not been subject to digital enhancement or bands removed by cropping. The original image is available as Supplementary File 2. (c) A representative image of bacteria from the multi-species community incubated with FITC-gelatin (green). The insert is a confocal 16S *r*RNA-FISH image showing the presence of *P. gingivalis* (red) and *P. micra* (blue) within the proteolytically-active bacterial clusters. The bar represents 10μm.

Figures

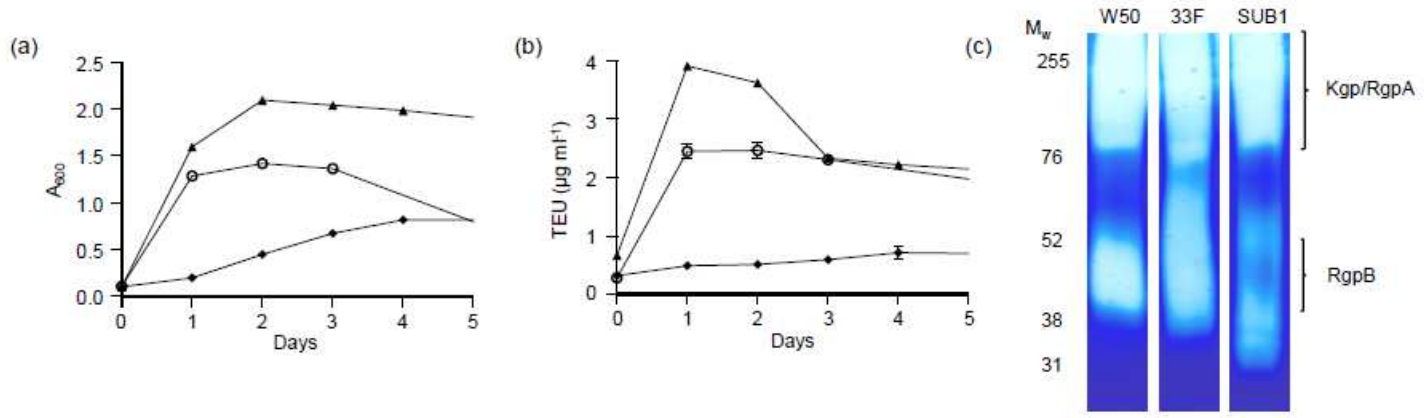

Figure 1. Growth and proteolytic activity of *P. gingivalis* strains in nutrient-rich broth

(a) Growth of strains [33F (▲), W50 (○) and SUB1 (◆)] in BHI over time was assessed as absorbance at 600nm and the graph shows mean ± sd of three independent biological replicates. (b) Proteolytic activity over time as assessed using a FITC-conjugated gelatin substrate and expressed as trypsin equivalent units (TEU). The graph shows mean ± sd of the same three independent biological replicates in (a). (c) Aliquots from the cultures on day 3 were subjected to zymography on gelatin-containing gels stained with Coomassie brilliant blue. All samples were run on the same gel and the image has not been subject to digital enhancement or bands removed by cropping. The original image is available in Supplementary File 1.

Figure 1

See image above for figure legend.

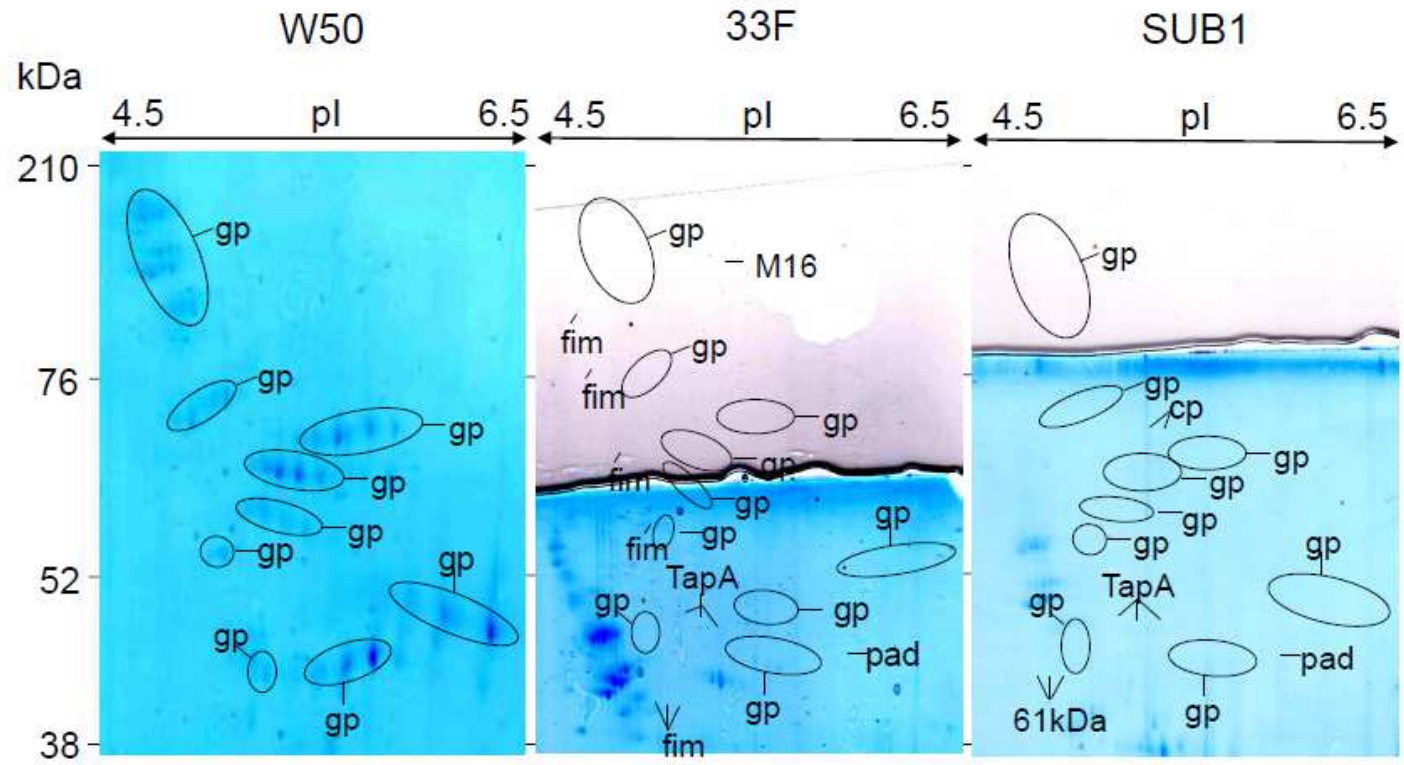

Figure 2

2DE gels of extracellular proteins from P. gingivalis strains Supernatants from cultures of P. gingivalis strains W50, 33F and SUB1 were subjected to 2D-PAGE and the gels stained with Coomassie brilliant blue. The major spots were excised and proteins identified using LC-MS/MS. Protein identities are presented in Table 1.

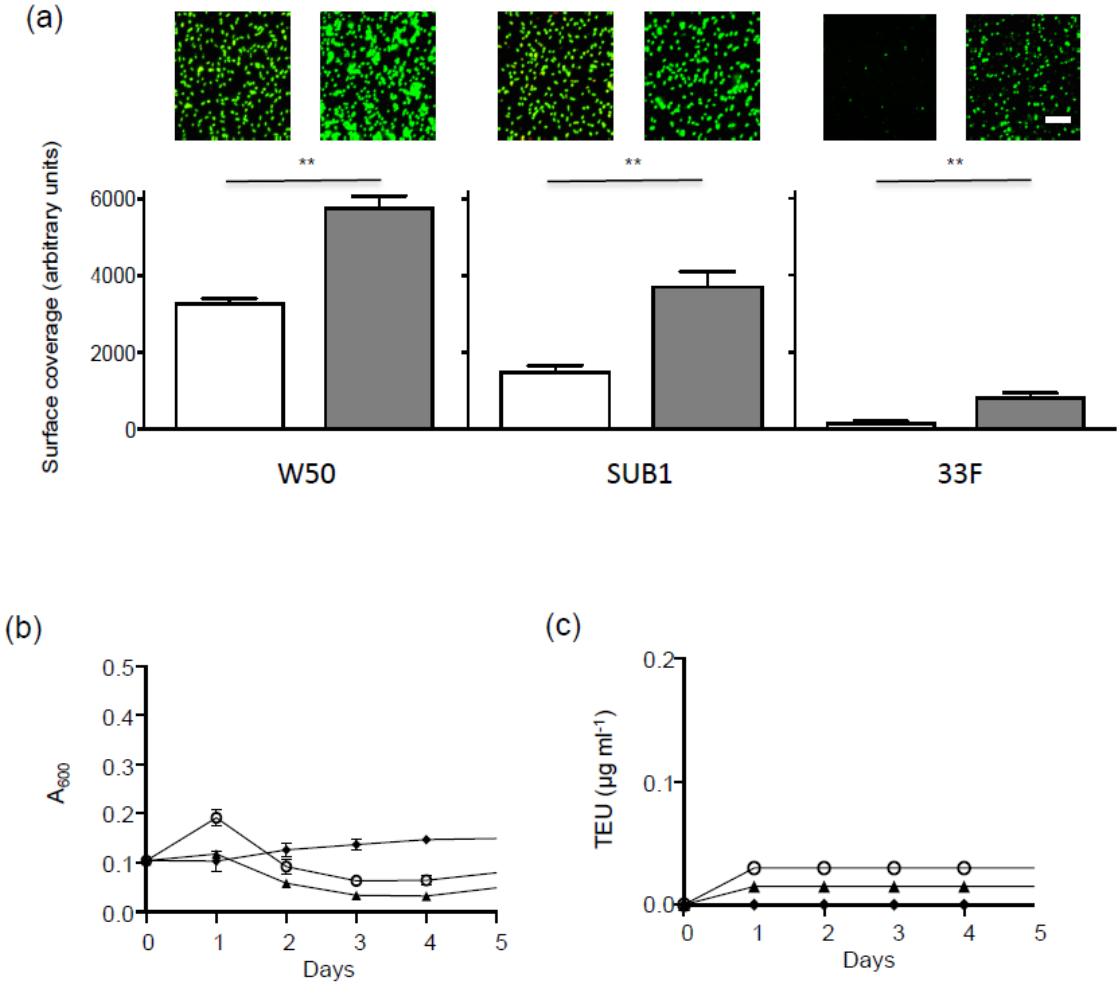

Figure 3. Survival of *P. gingivalis* strains in a serum environment

(a) Graphs showing coverage of *P. gingivalis* strains 33F, W50 and SUB1 on surfaces in the presence (■) or absence (□) of a serum coating. The bars show the mean ± sd of three independent biological replicates. Representative images show adherent bacteria stained with Baclight Live/Dead stain. The bar represents 10µm. **p<0.01. (b) Growth of *P. gingivalis* strains 33F (▲), W50 (❍) and SUB1 (◆) in serum, assessed as absorbance at 600nm. (c) Graph showing proteolytic activity of *P. gingivalis* strains W50 (❍), K1A (Δ) or E8 (●) in serum. The graph shows mean ± sd of three independent biological replicates.

Figure 3

See image above for figure legend.

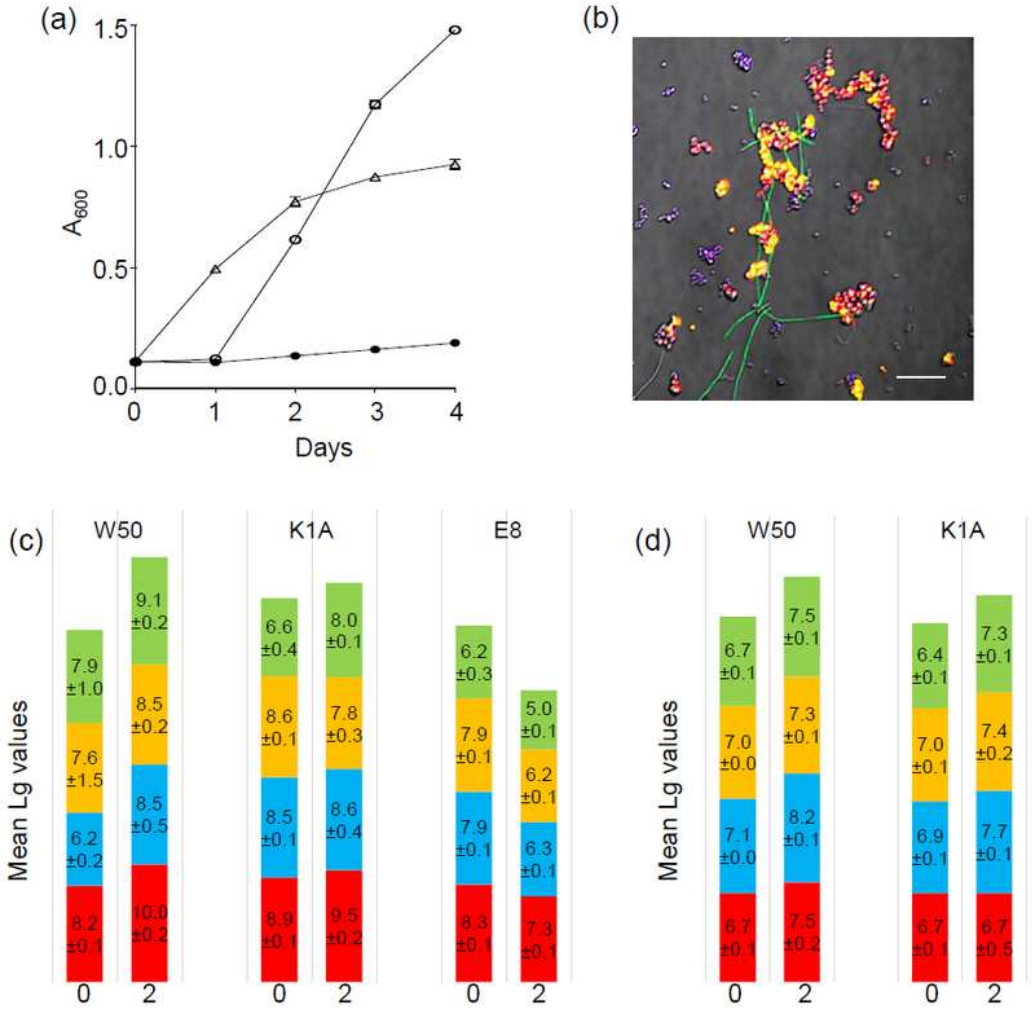

Figure 4. Growth and composition over time of multi-species communities containing *P. gingivalis* strains W50, K1A or E8 in serum

(a) Graph showing growth of multi-species communities containing *P. gingivalis* strain W50 (❍), K1A (Δ) or E8 (●) in serum, assessed as absorbance at 600nm (mean ± sd of three independent biological replicates). (b) A representative confocal FISH image showing composition of the W50-containing consortium after 2 days [*P. gingivalis* (red), *F. nucleatum* (green), *P. micra* (blue) and *S. constellatus* (yellow)]. The bar represents 10μm. Composition of multi-species communities containing *P. gingivalis* strains W50, K1A or E8 on day 0 and day 2 assessed using (c) growth on blood agar or (d) qPCR [*P. gingivalis* (red), *F. nucleatum* (green), *P. micra* (blue) and *S. constellatus* (yellow)]. Numbers represent mean ± sd of three independent replicates.

Figure 4

See image above for figure legend.

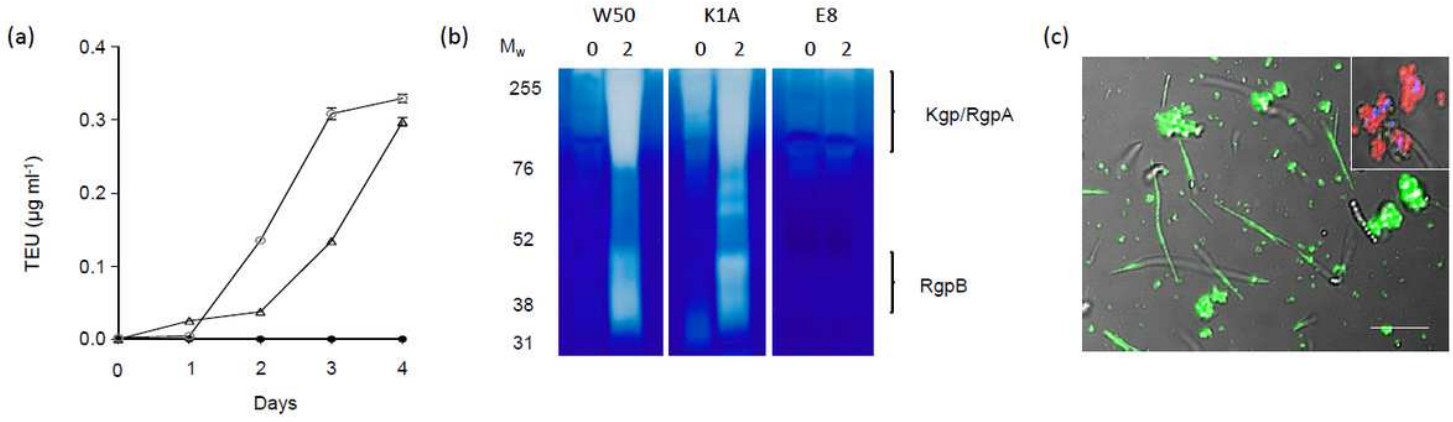

Figure 5. Proteolytic activity in multi-species communities containing *P. gingivalis* strains W50, K1A or E8 in serum

(a) Graph showing proteolytic activity of the multi-species communities containing *P. gingivalis* strains W50 (❍), K1A (Δ) or E8 (●) in serum. The graph shows mean ± sd of three independent biological replicates. (b) Aliquots (2µl) from the cultures on day 0 and day 2 were subjected to zymography on gelatin-containing gels stained with Coomassie brilliant blue. All samples were run on the same gel and the image has not been subject to digital enhancement or bands removed by cropping. The original image is available as Supplementary File 2. (c) A representative image of bacteria from the multi-species community incubated with FITC-gelatin (green). The insert is a confocal 16S *r*RNA-FISH image showing the presence of *P. gingivalis* (red) and *P. micra* (blue) within the proteolytically-active bacterial clusters. The bar represents 10µm.

Figure 5

See image above for figure legend.

Supplementary Files

This is a list of supplementary files associated with this preprint. Click to download.

- Suppl1.pptx
- Suppl2.pptx